Tellus (2002), 54B, 1–21
Printed in UK. All rights reserved

TELLUS
ISSN 0280–6509

Aircraft observation of carbon dioxide at 8–13 km altitude over the western Pacific from 1993 to 1999

By HIDEKAZU MATSUEDA*, HISAYUKI YOSHIKAWA INOUE and MASAO ISHII, *Geochemical Research Department, Meteorological Research Institute, 1-1 Nagamine, Tsukuba-shi, Ibaraki-ken 305-0052, Japan*

(Manuscript received 27 March 2001; in final form 10 September 2001)

ABSTRACT

The spatial and temporal variations of atmospheric CO_2 at 8–13 km from April 1993 to April 1999 were observed by measuring CO_2 mixing ratios in samples collected biweekly from a commercial airliner between Australia and Japan. The CO_2 growth rate showed a considerable interannual variation, with a maximum of about 3 ppm yr^{-1} during late 1997. This variation is related to the El Niño/Southern Oscillation (ENSO) events. A year-to-year change related to the ENSO events was also found in the latitudinal distribution pattern of the CO_2 annual mean between 30°N and 30°S. The averaged CO_2 seasonal cycle in the Northern Hemisphere gradually decayed toward the equator, and a relatively complicated variation with a double seasonal maximum appeared in the Southern Hemisphere. A significant yearly change of the seasonal cycle pattern was observed in the Southern Hemisphere. The impact of a tropical biomass-burning injection on the upper tropospheric CO_2 was estimated on the basis of the CO data from the same airliner observation.

1. Introduction

Carbon dioxide (CO_2) in the atmosphere has been increasing since the beginning of the industrial era due to human activities such as fossil-fuel burning and deforestation. Its increase will very likely cause future global climate changes as a result of the greenhouse effect of CO_2. Roughly half of the CO_2 emitted by burning fossil fuel accumulates as an airborne fraction, but this fraction largely depends on interannual variations of CO_2 uptake by the land biosphere and ocean (e.g., Keeling et al., 1989; Conway et al., 1994). Recently, interannual variations in the partitioning of fossil-fuel CO_2 have been estimated by various methods in conjunction with global carbon-cycle models on the basis of observational data (Francey et al., 1995; Keeling et al., 1995; Lee et al., 1998; Rayner et al., 1999a; Battle et al., 2000; Bousquet et al., 2000). Since these estimations are not completely accurate, more observations are needed to be able to constrain the fate of fossil-fuel CO_2 with accuracy by the use of global carbon-cycle models.

Atmospheric CO_2 mixing ratios have been measured by a large number of ground-based stations and cruise ships around the world (e.g., Conway et al., 1994; Keeling et al., 1995; Nakazawa et al., 1997b). In comparison with the global monitoring network in the surface air, CO_2 measurements above the planetary boundary layer (PBL) are sparse due to the limited number of high-mountain monitoring stations such as Mauna Loa in Hawaii (Conway et al., 1994). More information about the spatial variabilities of CO_2 above the PBL have been obtained by aircraft observations. Flask sampling using aircraft was performed to examine vertical and horizontal

* Corresponding author.
e-mail: hmatsued@mri-jma.go.jp

distributions of CO_2 over Japan (Tanaka et al., 1987a; Nakazawa et al., 1993), Australia (Pearman and Garratt, 1973; Pearman and Beardsmore, 1984; Pak et al., 1996), the western Pacific (Nakazawa et al., 1991; Matsueda and Inoue, 1996), USA (Tans et al., 1996), Europe-tropics (Brenninkmeijer et al., 1999), Antarctica (Murayama et al., 1995), and northern high-latitude regions around North America, Scandinavia and the Arctic (Bischof, 1962; Keeling et al., 1968; Bolin and Bischof, 1970; Bischof, 1971; Conway et al., 1985; Conway and Steele, 1989; Nakazawa et al., 1997a). Aircraft campaigns using on-board measuring systems also provided a detailed CO_2 distribution in the free troposphere (Wofsy et al., 1988; Anderson et al., 1993; Anderson et al., 1996; Boering et al., 1996; Hintsa et al., 1998; Zahn et al., 1999). Balloon platforms were also used to observe CO_2 vertical profiles from the troposphere to the stratosphere (Bischof et al., 1985; Schmidt and Khedim, 1991; Nakazawa et al., 1995; Harnisch et al., 1998; Ray et al., 1999; Strunk et al., 2000). Expense and the short-term nature of aircraft campaigns mean that temporal and spatial variabilities of CO_2 above the PBL have not been well defined on a global scale in comparison with surface air measurements.

To deduce the global sink and source distributions of CO_2, most atmospheric three-dimensional (3-D) transport models were based mainly on a comparison with the CO_2 observational data in the lower troposphere. It has been pointed out that not only lower tropospheric data but also aircraft data are available to validate the simulated results of middle and upper tropospheric CO_2 variations by transport models (Law and Simmonds, 1996; Taguchi, 1996; Craig et al., 1998). Upper tropospheric data could improve atmospheric CO_2 transport processes such as convection, interhemispheric transport in the upper troposphere, and exchange between the upper troposphere and the lowermost stratosphere (e.g., Strahan et al., 1998). Thus, more systematic and long-term measurements of CO_2 in the free troposphere and the lowermost stratosphere are necessary for a better evaluation of a global carbon cycle model for atmospheric CO_2.

A commercial airliner is useful for collecting CO_2 data in the upper troposphere (e.g., Pearman and Beardsmore, 1984; Nakazawa et al., 1991). An airliner observation over the western Pacific between Australia and Japan was carried out for two years in 1984 and 1985 by Nakazawa et al. (1991). Although no systematic measurement along this flight route was taken during 1986–1992, our airliner observations started in 1993 to obtain a long-term measurement of CO_2 over the same western Pacific area. To observe for a longer period of time, improvements based on the manual air sampling method used by Nakazawa et al. (1991) were required to establish an automated sampling system. Thus, we developed a new automatic flask sampling system as airborne equipment for a commercial airliner (Boeing 747) under a co-operative program with the Meteorological Research Institute (MRI), the JAL Foundation, Japan Airlines (JAL), the Japan Meteorological Agency (JMA), and the Japanese Ministry of Land, Infrastructure and Transport. The operation of the sampling system started in April 1993 using a JAL passenger aircraft between Australia and Japan to measure the mixing ratios of trace gases such as CO_2, methane (CH_4) and carbon monoxide (CO) at 8–13 km. Previous results of CO_2 measurements for 1 yr from April 1993 to April 1994 were reported to describe seasonal cycles and their latitudinal change over the western Pacific (Matsueda and Inoue, 1996). We continued the JAL airliner observations to clarify long-term variations of the trace gas mixing ratios in the upper troposphere, and this observation is ongoing. In this paper, we present a 6-yr record of the CO_2 mixing ratio from 1993 to 1999 on the basis of new data for 5 years combined with the previous measurements for 1 yr. First, the observed CO_2 data are analyzed to clarify a latitudinal difference in the time variations for 12 latitudinal bands from 30°N to 30°S over the western Pacific. Second, growth rates, latitudinal distributions, and seasonal cycles are examined to identify their interannual variations during 6 yr. In particular, we discuss several possible causes for the CO_2 interannual variation, focusing on the large anomaly between 1997 and 1998.

2. Experimental procedures

2.1. Flask sampling

Since details of our flask sampling for the commercial airliner (Boeing 747) have been reported elsewhere (Matsueda and Inoue, 1996;

Matsueda et al., 1998), only a brief description of the sampling procedure is given here. The Automatic air Sampling Equipment (ASE) consists of 12 titanium flasks with an internal volume of about 1.9 L. Several test flights demonstrated that sampled air from the air-conditioning system was collected without any contamination, as described below. A similar result for the Boeing 747 air sampling has also been reported by Nakazawa et al. (1991). The flask sampling was operated automatically by a main control unit attached to the ASE without any assistance from crew members. Each sample flask was completely flushed using a metal bellows pump, and then air was pressurized into the flask. The sampling time for each flask could be recorded in the main control unit to determine the location and altitude of the sampling point by comparison with the flight record from the aircraft navigation system.

Between April 1993 and April 1999, 126 northbound sampling flights were made using the Boeing 747 passenger aircraft of Japan Airlines (JAL) from Australia to Japan (Fig. 1). The reason for this was that northbound flights are better than southbound flights at minimizing the storage time of sampled air in the flask before analysis. The longitudes of the sampling points ranged from 140°E to 152°E, although, exceptionally, some flights had to divert from the main route slightly due to weather conditions. Detailed information about the latitudes and altitudes of all sampling points is shown in Fig. 2. For each flight, 12 air samples were collected every 30–41 min, which corresponded to a latitudinal interval of about 5–6°. The first 12 flights before June 1994 were made once a month from Cairns, Australia (16°53′S, 145°45′E) to Narita, Japan (35°46′N, 140°23′E). After July 1994, the flight route changed from Cairns to Sydney (33°58′S, 151°11′E) to expand the latitudinal coverage of the sampling points in the Southern Hemisphere from 13°S to 30°S. In addition, the frequency of sampling flights increased from once to twice a month since July 1994. At least one flight was made each month, except for September 1993 and March 1995, due to a major re-arrangement of the aircraft. The air samples were collected at the cruising altitudes of 8–13 km, although four samples were exceptionally obtained at altitudes lower than 8 km during descents near Narita International Airport (Fig. 2b). It is noted that the sampling altitudes of about 9–11 km in the Southern Hemisphere were systematically lower than those of 10–12 km in the Northern Hemisphere (Fig. 2c) because the cruising altitude for the northbound flight usually jumped up at around 10°S. The sampling altitude depended on the cruising altitudes for each flight, but no periodic change such as a seasonal or interannual cycle was found in the sampling altitude. This fact indicates that seasonal and interannual variations of CO_2 observed in this study are not induced by the periodic change of the sampling altitude.

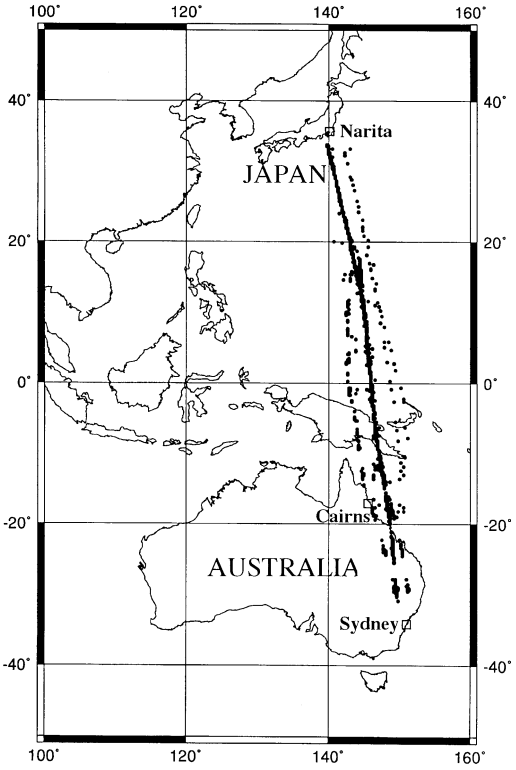

Fig. 1. Locations of flask air samples collected from northbound flights from Australia to Japan between April 1993 and April 1999. The sampling flights from 23 April 1993 to 23 June 1994 were from Cairns in Australia to Narita in Japan, while the later flights after 27 July 1994 were from Sydney to Narita. Details on the latitudes and altitudes of all sampling locations are provided in Fig. 2. The map was created with GMT-3 (Wessel and Smith, 1991).

2.2. *Analytical methods*

The ASE with sampled air in the flasks was removed from the aircraft just after arrival at the

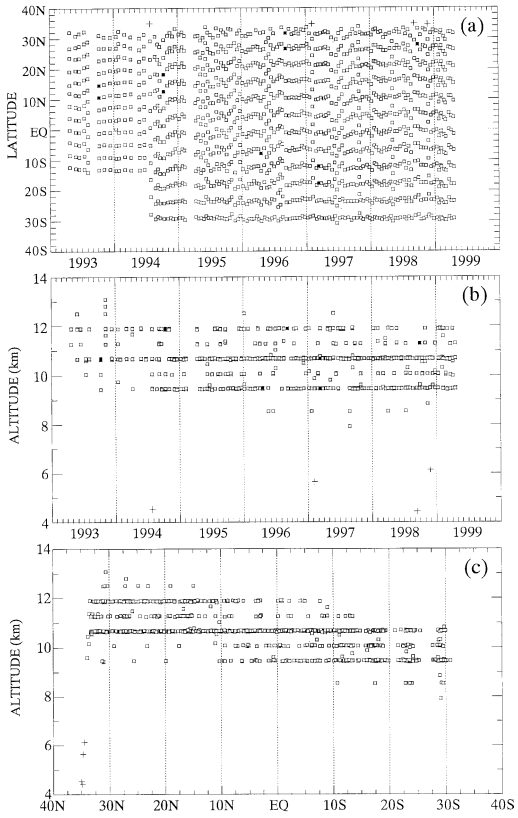

Fig. 2. Latitudes (a) and altitudes (b) for flask samples from 126 flights between April 1993 and April 1999 as well as latitudinal distribution of the sampling altitudes (c). The solid squares and crosses represent rejected samples, the measurements of which were not used for time-series data analysis (see text).

Narita International Airport, and was then transported to the Meteorological Research Institute/Geochemical Research Department (MRI/GRD) for trace gas analysis. The analysis of CO_2 was immediately conducted for all flask samples within 30 h after collection to prevent a change in the mixing ratio. Several storage tests indicated no significant drift of CO_2 content in any flasks until analysis.

The ASE was connected to a trace gas measuring system and automatically operated by a laboratory computer for sample introduction and analysis of all flask samples. The CO_2 mixing ratio was measured using a nondispersive infrared gas analyzer (NDIR; Binos 4.1b, Rosemount). Prior to the NDIR analysis, the sampled air was completely dried using a chemical desiccant [$Mg(ClO_4)_2$]. CO_2 was measured only once for each flask sample, but standard gases were analyzed before each sample measurement so that the NDIR precision for six sample analyses in succession could be evaluated. The standard deviations for six repetitive analyses of standard gases ranged within less than 0.08 ppm with a mean of about 0.02 ppm. The analytical precision was almost constant for 6 yr from April 1993 to April 1999. Thus, the analytical stability for our NDIR system was maintained over this period of time.

The CO_2 mixing ratio in the sampled air was determined by five standard gases of CO_2 in air with a range from about 330 to 390 ppm. Two sets of five standard gases were used from 1994 to 1999 with an exchange in January 1997. All standard gases based on purified natural air were prepared in 48-L aluminum or 47-L steel cylinders by the volumetric method used at a gas company (Nippon Sanso Co., Japan). Their CO_2 mixing ratios were calibrated twice per year at JMA by using the secondary standard gases assigned by the WMO CO_2 standard gas scale. Thus, the CO_2 mixing ratios in all air samples are reported here on the basis of the WMO CO_2 mole fraction scale. This CO_2 scale was propagated from the primary standard gases of JMA, of which mixing ratios were assigned in 1999 by WMO Central CO_2 Laboratory operated by the National Oceanic and Atmospheric Administration/Climate Monitoring and Diagnostics Laboratory (NOAA/CMDL). The previous results for one year from 1993 to 1994 were reported on the basis of the WMO 85-x scale (Matsueda and Inoue, 1996), but they were re-calculated in this study to make them uniform by the adoption of the WMO CO_2 mole fraction scale.

To evaluate the long-term stability of our standard gases, internal consistency among five standard gases was examined using the same method as described by Matsueda et al. (1998). The CO_2 mixing ratio of each standard gas was calculated based on the measurements of the other four standard gases to estimate the magnitude of the drift. All standard gases in the first set showed no significant change of CO_2 mixing ratio (less than ± 0.02 ppm yr^{-1}) from April 1993 to January 1997. Such stability for these standard gases was also confirmed by the results from the regular calibration experiments at JMA. In the second set

of standards used after January 1997, a large drift with about 0.2 ppm yr^{-1} was found in one cylinder, but the other four cylinders were stable. The estimated drift was taken into account for the calculation of the CO_2 mixing ratios in the sampled air, while another calculation was made using measurements of the four standard gases without the drift cylinder. The difference between the calculations was not significant, being less than ± 0.02 ppm. In the present study, the latter method without the drift standard gas was used for calculating the CO_2 mixing ratios in the sampled air after January 1997. Taking into account the possibility for error in calculation and analysis, the overall precision was estimated to be less than 0.1 ppm in the present study.

3. Results

About 1500 flask air samples were collected during 126 flights between April 1993 and April 1999 and analyzed for CO_2 mixing ratios. Fourteen flask samples for four flights were not collected because of a failure of the sampling equipment. The measured CO_2 mixing ratios in all air samples were carefully examined to ensure the high quality of the measurements according to the following procedures. First, analytical errors due to instability of the NDIR analyzer were evaluated on the basis of the precision of the measurements of five standard gases before and after sample analysis. Second, the CO_2 data were compared with other trace gas measurements such as CH_4 and CO in the same sampled air to check for sampling contamination due to a leakage of the pump and tubing. In addition, several comparison experiments between the sampled air and fresh air outside the aircraft were conducted to ensure that there was no change in the CO_2 content when passing through the air-conditioning system. Third, several flask storage tests were performed during this observational period of time to confirm that there was no drift of CO_2 content until analysis. We ensured through these quality assurance steps that the CO_2 mixing ratios in all sampled air could be measured with an overall uncertainty of less than 0.1 ppm.

Data analysis for the measurements was conducted to make time-series data sets of mean CO_2 for 12 latitudinal bands at intervals of 5° latitude between 30°N and 30°S, and their results are shown in Fig. 3. These analyzed data represent the time variations between 8 and 13 km assuming no significant vertical gradient of CO_2 mixing ratio within these altitudes, although the mean altitude was slightly different between the Northern and Southern Hemispheres, as described above. In addition, a small longitudinal difference in the flight routes between Cairns–Narita and Sydney–Narita was ignored here. The measurements at about 13 km around Japan were occasionally influenced by the intrusion of lower stratospheric air in the boreal winter (Nakazawa et al., 1991; Matsueda and Inoue, 1996). It was difficult to ascertain whether the measurements were from the troposphere or not because the tropopause height near Japan is highly variable in winter. In the present study, the measurements were not selected from the point of view of the tropopause level. Thus, the influence of stratospheric air on the CO_2 variation is included near Japan.

The data analysis for Fig. 3 was performed according to a procedure similar to that described by Matsueda and Inoue (1996). First, latitudinal distribution from the CO_2 measurements for each flight was fitted by a cubic spline function to obtain interpolated values for the 1° latitude. Four exceptional measurements at altitudes lower than 8 km were not used here. In addition, eight measurements for four flights were excluded from the spline fittings because they were identified to be directly influenced by the strong intrusion of continental air masses, as reported by Matsueda and Inoue (1996). Such rejected measurements were largely deviated from the final fitting curves for the smoothed CO_2 variations, as clearly shown in Fig. 3. Second, the equally spaced data for the 1° latitude from the spline fittings were used to calculate the mean CO_2 mixing ratios for 12 latitudinal bands at intervals of 5° latitude between 30°N and 30°S. Third, the mean data for each latitudinal band were analyzed by a curve fitting for the components of both the increasing trend and the seasonal cycle. Both components were approximated by fitting a linear function combined with three harmonics as follows:

$$f(t) = a_1 + a_2 t + \sum_{i=1}^{3} \times [a_{2i+1} \sin(2\pi i t) + a_{2i+2} \cos(2\pi i t)], \quad (1)$$

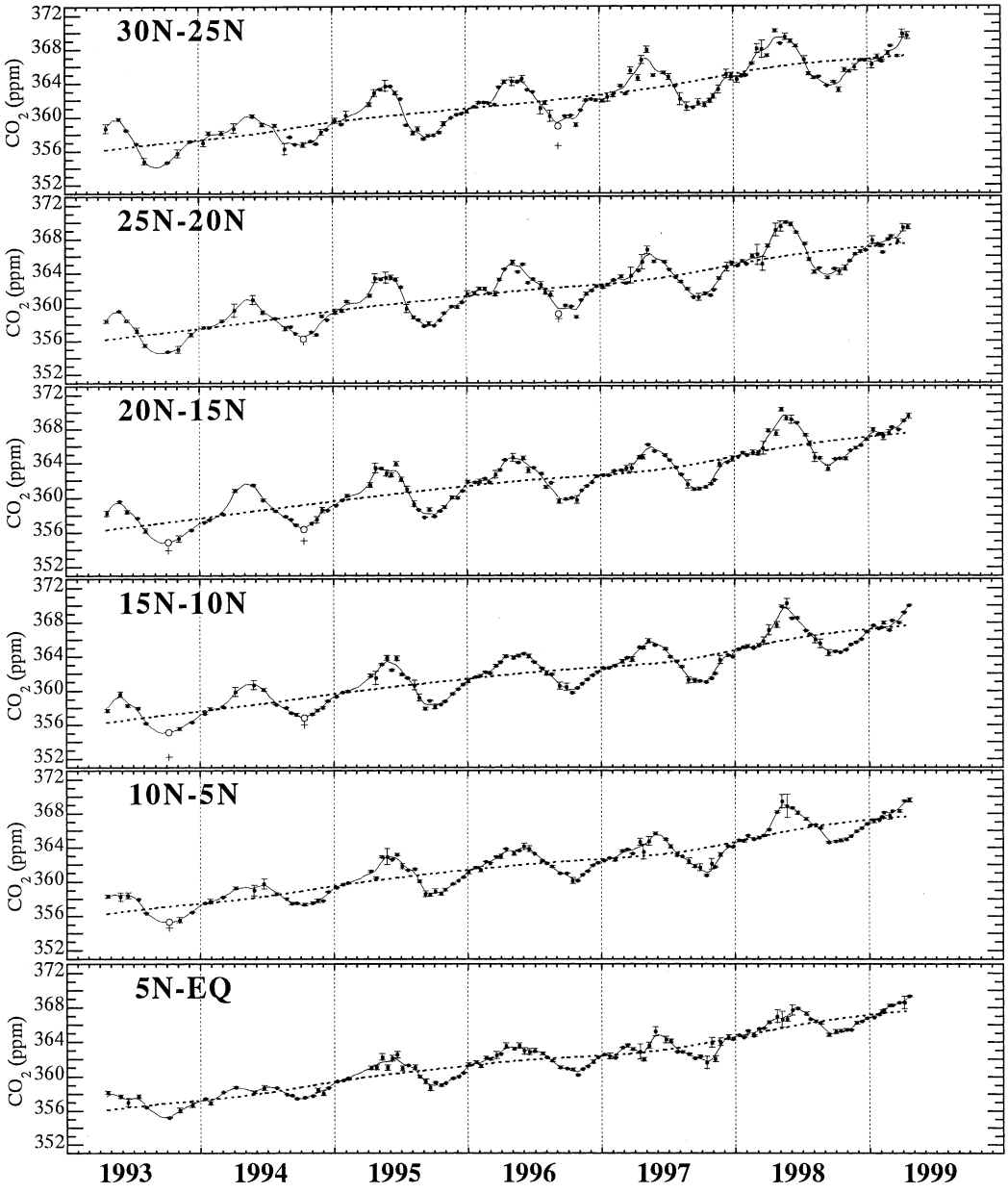

where t is the elapsed time and the values of a_i are defined by the fitting. Fourth, the differences between the fitting curve by eq. (1) and the data (residuals) were fitted to the cubic spline function to obtain equally spaced residuals at about 1-week intervals. These residuals were smoothed by applying a low-pass filter that reduced variations on time scales less than $\sim$40 days. The final fit consisted of the sum of the linear term, the harmonics, and the filtered residuals. The mean difference between the data and the final fitting curve was 0.26 ppm. On the basis of the final

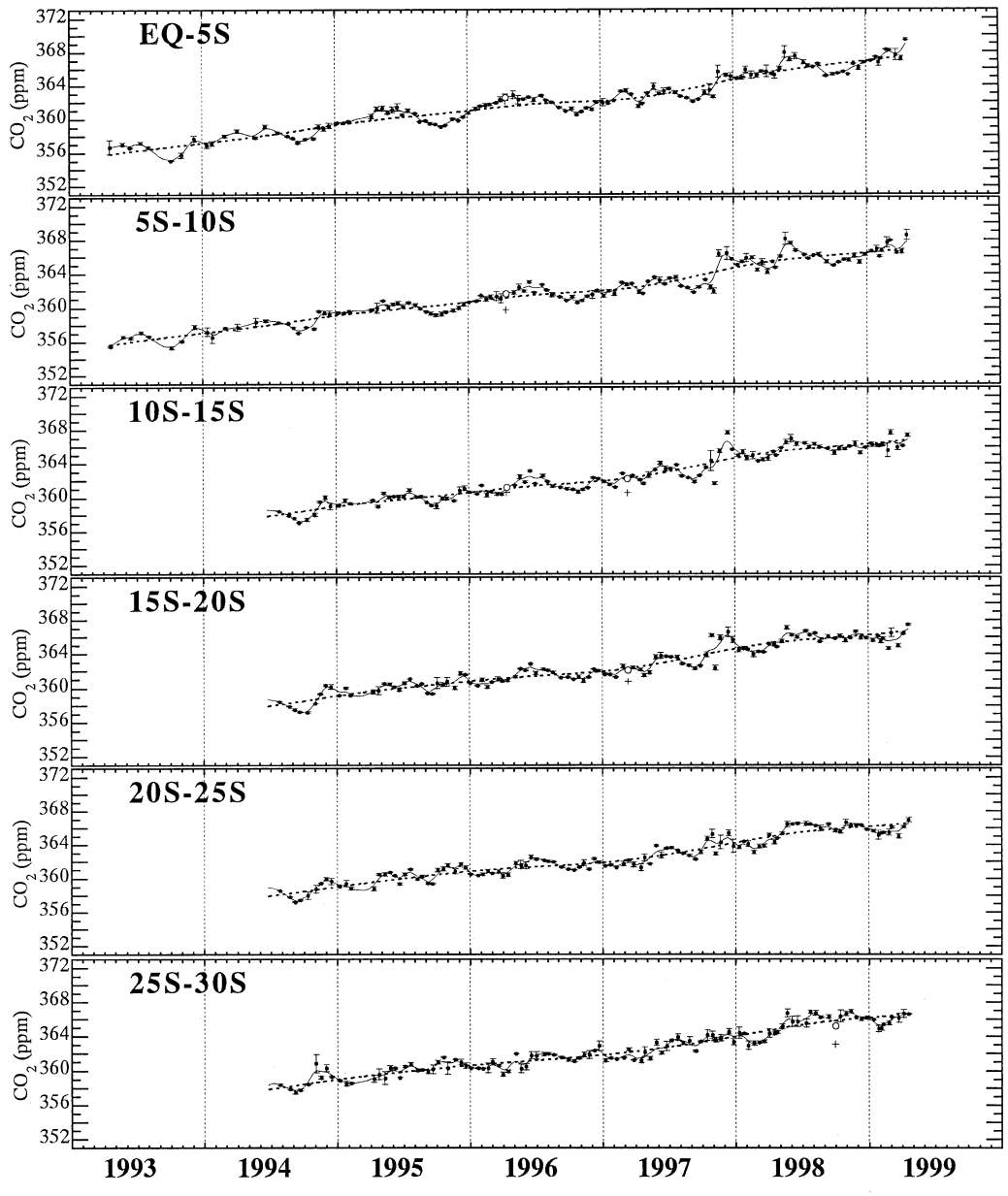

Fig. 3. The time variations of CO_2 mixing ratios divided into 12 latitudinal bands from 30°N to 30°S observed at 8–13 km over the western Pacific from April 1993 to April 1999. Each piece of data represents the mean CO_2 mixing ratio for 5° latitude calculated from the measurements, and its error bar is ± 1 standard deviation of the mean. The crosses and open circles represent the means before and after data selection, respectively. The solid and dashed curves represent the smoothed-fit curve and long-term trend, respectively. The procedure for data analysis is described in detail in the text.

fitting curve, annual mean CO_2 mixing ratios were calculated for 12 latitudinal bands between 30°N and 30°S (Table 1). On the other hand, the residuals were smoothed by applying a low-pass filter that reduced variations on timescales less than 1.5 yr. These filtered residuals were added to the linear term to make a long-term trend curve, as shown in Fig. 3.

4. Discussion

4.1. Growth rate

The long-term trend showed a continuous increase of CO_2 level from April 1993 to April 1999 in all latitudinal bands between 30°N and 30°S. Figure 4 shows CO_2 growth rates for 12 latitudinal bands which were calculated from the derivatives of the trend fitting curves in Fig. 3. The growth rate during this observational period of time shows a large interannual variation with a pattern that was similar in all latitudinal bands. However, it is of interest that the phase of the interannual variation of the CO_2 growth rate largely depended on latitudes. In particular, such a phase difference with latitude was clearly found in the largest growth rate from late 1997 to early 1998. The time lag of the growth rate peak during 1997–1998 was about 6 months for the latitudinal range between 30°N and 30°S. The growth rate

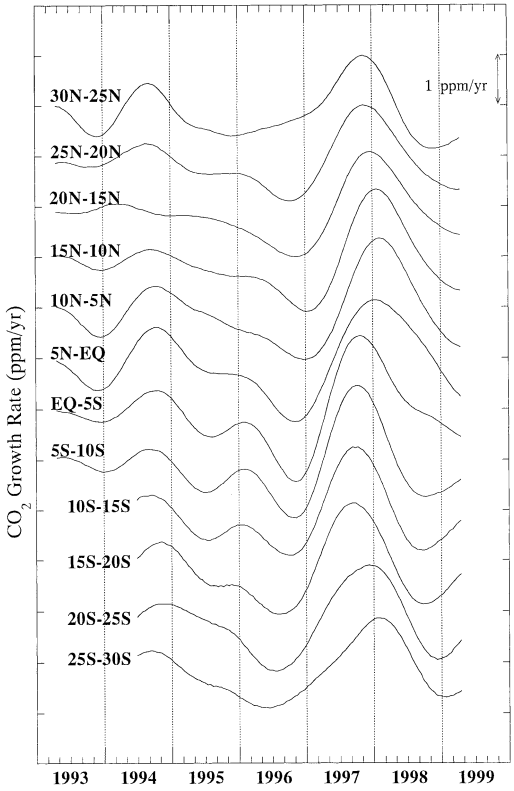

Fig. 4. The time variations of CO_2 growth rates for 12 latitudinal bands from 30°N to 30°S observed at 8–13 km over the western Pacific.

Table 1. *Mean altitudes for air samples, annual mean CO_2, and residuals for 12 latitudinal bands between 30°N and 30°S from 1994 to 1998*

Latitudes	Mean altitude (km)	Annual mean CO_2 (ppm)					Residual (ppm)
		1994	1995	1996	1997	1998	
30°N–25°N	11.3	358.2	360.3	361.8	363.6	366.3	0.33
25°N–20°N	11.2	358.5	360.4	362.0	363.5	366.2	0.28
20°N–15°N	11.1	358.7	360.5	362.1	363.3	366.1	0.24
15°N–10°N	11.0	358.6	360.5	362.2	363.3	366.2	0.20
10°N–5°N	10.7	358.3	360.5	362.1	363.3	366.2	0.20
5°N–0°	10.6	358.1	360.4	362.0	363.1	366.0	0.21
0°N–5°S	10.6	358.1	360.1	361.8	363.0	365.9	0.23
5°S–10°S	10.5	358.0	359.9	361.5	363.0	365.7	0.27
10°S–15°S	10.2		359.9	361.4	363.1	365.6	0.28
15°S–20°S	10.0		360.1	361.4	363.2	365.6	0.29
20°S–25°S	9.8		360.1	361.4	362.9	365.5	0.25
25°S–30°S	9.6		359.9	361.2	362.7	365.3	0.28

The annual mean CO_2 was calculated by the fitting curve, while the residual represents a mean difference between the fitting curve and observed data.

peak first appeared in the southern tropical regions between 5°S and 20°S in August–September 1997. It was gradually delayed toward the north and the south. In the Northern Hemisphere, the appearance of the maximum growth rate was the latest at the latitudinal band between 5°N and 10°N in January–February 1998, and then it gradually hastened toward 30°N. It has been reported that the lower tropospheric CO_2 also showed a similar phase shift in growth rate as that of the earliest peak in the tropical regions (Conway et al., 1988; Conway et al., 1994), although their results were obtained in an earlier time period than that presented here. The other increased peak of the growth rate was also observed in late 1994, but the phase shift with latitude during this period was not well defined because of the lack of observed data south of 10°S before July 1994.

Figure 5a shows mean growth rates in the Northern (30°N–0°) and Southern (30°S–0°) Hemispheres calculated from averages of the growth rate variabilities for six latitudinal bands in the two semihemispheres. The overall growth rate from April 1995 to April 1998 was similar in magnitude for both hemispheres, and its average was calculated to be about 1.8 ppm yr^{-1}. In comparison with past CO_2 levels of about 344 ppm in 1984 and 345 ppm in 1985 in the upper troposphere over the same western Pacific (Nakazawa et al., 1991), our recent results clearly show an elevation of 14–15 ppm in the CO_2 level during the past 10 years. This average of the CO_2 increase rate in the upper troposphere is quite similar to that of 1.43 ppm yr^{-1} in the surface air averaged during a similar period from 1981 to 1992 (Conway et al., 1994). Compared to the past decadal average from 1980s to early 1990s, the recent growth rate during the late 1990s showed a higher average for the CO_2 growth rate. This is caused by significantly increased growth rates around 1994/95 and 1997/98 during the observational period.

The variabilities of the mean growth rates in both hemispheres ranged from about 1 ppm yr^{-1} to 3.0 ppm yr^{-1} during 1993–1999 (Fig. 5a). This interannual variability showed a relatively increased growth rate to about 2.2 ppm yr^{-1} in late 1994 and a gradual decline from 1995 to 1996. At about 1 ppm yr^{-1}, the growth rate in late 1996 was the lowest and then increased rapidly to a maximum of more than 3 ppm yr^{-1} in late 1997. Although there is uncertainty concerning the rapid decrease of the growth rate in 1998 due to the end effects associated with the curve-fitting procedure, a preliminary analysis of available data until 2000 suggests that the qualitative features of the rapid decline around 1998 will not change drastically when the data in 2000 are included. In the lower troposphere, a similar extremely increased growth rate of more than 3 ppm yr^{-1} was also observed

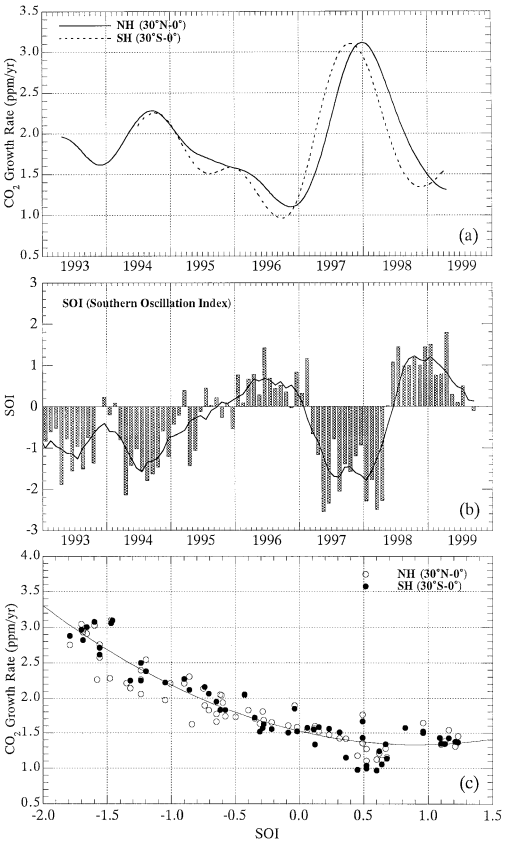

Fig. 5. (a) The time variations of mean CO_2 growth rates in two hemispheres from 1993 to 1999. The solid and dashed lines represent the Northern (30°N–0°) and Southern (30°S–0°) tropics, respectively. (b) The monthly mean of the Southern Oscillation Index (SOI) from 1993 to 1999 with the 7-month running mean (solid curve). (c) The relationship of the monthly mean data between the CO_2 growth rate and SOI. A phase delay of 3 months was corrected for the growth rates in the Northern tropic. The solid line represents the best-fit curve by a quadratic equation to all data points ($y = 1.53 - 0.424x + 0.234x^2$, $r = 0.937$).

around early 1998 by the JMA monitoring stations in the western North Pacific (Watanabe et al., 2000) and the global sampling network of the NOAA/CMDL (Bell et al., 1999). Similar variability of the growth rate between the free troposphere and the surface air was reported by previous aircraft observations over southeastern Australia (Pearman and Beardsmore, 1984) and over Japan (Tanaka et al., 1987a; Nakazawa et al., 1993). These results indicate that the large increase of the growth rate around 1997–1998 is a global-scale phenomenon.

The interannual variation of CO_2 growth rates in both hemispheres is associated with the El Niño/Southern Oscillation (ENSO) events that are described by the Southern Oscillation Index (SOI) in Fig. 5b. The SOI used here is defined as the sea level pressure anomaly difference between Tahiti and Darwin divided by the standard deviation in the 30-yr period from 1961 to 1990 (Japan Meteorological Agency, 1999). The significant enhancement of the CO_2 growth rate in late 1997 appeared during the strongest El Niño event from 1997 to 1998. A growth rate increase was also found during an El Niño year in 1994, but the CO_2 in the weak La Niña year of 1996 showed a large decline of the growth rate. Such interannual variation relating to the ENSO events is well known in the CO_2 record in the surface air (e.g., Bacastow, 1976; Bacastow et al., 1980; Keeling et al., 1989; Thompson et al., 1986; Conway et al., 1988; Elliott et al., 1991). Thus, the growth rate variability in the upper troposphere is primarily caused by the yearly change in the CO_2 uptake by the land biosphere and ocean due to the ENSO events (e.g., Francey et al., 1995; Keeling et al., 1996a; Lee et al., 1998; Rayner et al., 1999b; Battle et al., 2000). Compared with two strong ENSO events in 1997/98 and 1982/83, there were some differences in the growth rate variability. During the 1997/98 ENSO event, the growth rate maximum showed a similar value between the Northern and Southern semihemispheres (Fig. 5a). However, the growth rate maximum during the 1982/83 ENSO event showed a large difference between the two semihemispheres (Conway et al., 1994). In addition, the growth rate maximum in the 1997/98 ENSO event was about 1 ppm larger than that of the 1982/83 ENSO event (about 2 ppm yr^{-1}). These differences suggest that the pattern of the CO_2 growth rate variability and its cause differ between ENSO events. It has also been pointed out that there are some differences in the growth rate variability between the 1982/83 and 1986/87 ENSO events (Conway et al., 1994). One possible cause is the yearly changes in the regional CO_2 fluxes from land and oceans, which was evaluated by an inverse model study on the basis of CO_2 measurements for 20 yr (Bousquet et al., 2000).

During the 1997/98 ENSO event, the growth rate maximum clearly showed a phase difference between the Southern and Northern Hemisphere (Fig. 5a). As a result of this phase difference, no significant time lag between the growth rate and the SOI variabilities was found in the Southern Hemisphere, but the growth rate in the Northern Hemisphere was delayed for about 3 months compared to the phase of the SOI. In the lower troposphere, the correlation between the growth rate and the ENSO cycle showed a mean phase lag for about 7 months by the NOAA/CMDL global sampling network from 1981 to 1984 (Conway et al., 1988), although there is a tendency for the lags to be shorter near the equator and longer toward the poles. A similar phase lag for about 6 months was observed at the JMA monitoring stations in the western North Pacific (24°N–39°N) from 1993 to 1998 (Watanabe et al., 2000). These results indicated that the growth rate peak in the upper troposphere appeared about 3 months earlier than that in the lower troposphere. This phase difference suggested an additional CO_2 input into the upper troposphere from biomass burnings enhanced during the ENSO event, which is discussed in detail in Section 4.4. To examine the detailed relationship between the growth rate and SOI, the monthly means of the CO_2 growth rates in the both hemispheres were plotted against the monthly mean SOI values (Fig. 5c). The monthly mean SOI used here was calculated by the smoothed curve of the 7-month running mean in order to remove the short-term variability. When the phase delay by 3 months was corrected for the data in the Northern Hemisphere, all of the data in both hemispheres showed a strong negative relation between the growth rate and SOI. This empirical relation was almost described as a quadratic function to show an accelerated increase of the growth rate with a stronger ENSO event during 1993–1998.

4.2. Latitudinal distribution

Figure 6 shows latitudinal distributions of the annual mean CO_2 between 30°N and 30°S for 5 yr from 1994 to 1998. The annual mean was relatively higher in the Northern Hemisphere than it was in the Southern Hemisphere. A mean difference between the maximum and minimum was estimated to be about 0.8 ppm between 30°N and 30°S. The minimum appeared in the latitudinal band between 25°S and 30°S every year, but the latitudes for the maximum peak in the Northern Hemisphere largely depended on the year. Thus, the latitudinal distribution pattern clearly showed a year-to-year change over the western North Pacific.

The annual means in 1995 and 1996 show a quite similar distribution with a maximum at the northern tropical regions around 10°N. This pattern for both years was similar to previous results observed for 1984 and 1985 in the upper troposphere over the same western Pacific (Nakazawa et al., 1991). In contrast, a different pattern with no clear maximum at the northern tropical region was found in 1997. The CO_2 distributions in 1998 and 1994 also showed a slightly perturbed pattern with a different shape of the northern tropical peak compared to those in 1995/96. These differences suggest that a yearly change of the CO_2 latitudinal distribution is related to the El Niño events in 1997/98 and 1994 because the northern tropical maximum was found only during the non-El Niño years of 1995/96 and 1984/85. A change in the tropical distribution pattern during the El Niño years was also observed in the lower tropospheric CO_2 (Conway et al., 1988; Keeling et al., 1989). Nakazawa et al. (1991) pointed out that the northern tropical maximum in the upper troposphere may appear due to an upward transport of the lower tropospheric air near the Intertropical Convergence Zone (ITCZ), which is usually located around 5°N in the western Pacific region. The satellite-derived climatology from the highly reflective cloud dataset indicates that the intensity of the ITCZ in the western Pacific is significantly weakened during the El Niño years due to the eastward shift of the convection center to the central Pacific (Waliser and Gautier, 1993). It has been suggested that suppressed upward transport at the ITCZ during the ENSO events may diminish a supply of high CO_2 from the surface air to the upper troposphere over the tropical western Pacific. Another possible cause is interannual variations in the CO_2 outflux from the equatorial Pacific Ocean, which were largely reduced during the ENSO events around 1994 and 1997/98 (Inoue et al., 1996; Feely et al., 1999). Thus, this lower oceanic outflux, combined with the suppressed upward transport in the tropical region, significantly contributes to the change of the northern distribution pattern during the ENSO events. In addition, a yearly change of stratosphere–troposphere exchange activity may influence the CO_2 annual mean in the northern mid-latitude because a difference in the CO_2 mixing ratio was observed between the upper troposphere and the lowermost stratosphere (e.g., Nakazawa et al., 1991).

In the Southern Hemisphere, the prominent feature of the latitudinal distribution is a local increase in the southern subtropical region between 15°S and 20°S in most years. A similar increase around 20°S was also seen in the previous

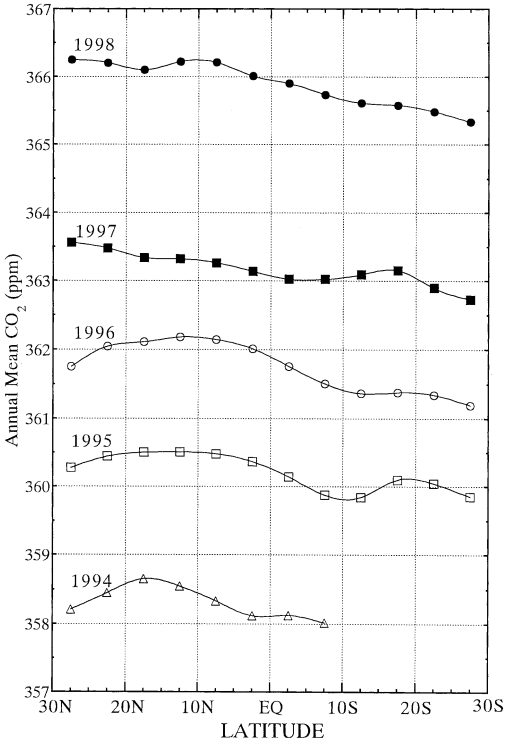

Fig. 6. Latitudinal distributions of annual mean CO_2 at 8–13 km during 1994–1998.

annual mean data for 1984 and 1985 in the upper troposphere over the same area of the South Pacific (Nakazawa et al., 1991). It has been suggested that high CO_2 from the surface air is transported upward and crowded into the southern subtropics. Carbon monoxide (CO) measurements from our airliner observation clearly showed a southern subtropical increase around 20°S during the austral spring due to a long-range transport of biomass-burning CO from the tropics into the upper troposphere near the southern subtropical jet stream (Matsueda et al., 1998; Matsueda et al., 1999). This fact suggests that CO_2 emitted from tropical biomass burnings is partly responsible for the local increase in the southern subtropics. On the other hand, Nakazawa et al. (1991) pointed out that upper tropospheric CO_2 in the Southern Hemisphere was influenced by the southward transport of the northern hemispheric air associated with the South Pacific Convergence Zone (SPCZ) and the monsoon circulation. These results suggested that the transport-induced change and biomass-burning emissions could affect the year-to-year variability in the southern subtropical peak.

Figure 7 compares data from the lower and middle troposphere to ours from the upper troposphere to clarify the vertical difference in the CO_2 annual mean. Data are plotted as relative to the surface mean at Cape Grim (40°41′S, 144°41′E) in Australia. The data used were obtained from the global observation network of NOAA/CMDL using ground-based stations and ships in the Pacific regions from 1994 to 1997 (Tans et al., 1996; Tans et al., 1998), and aircraft observation over southeast Australia from 1992 to 1997 by the Bureau of Meteorology and the CSIRO Division of Atmospheric Research (Pak, 2000). To show the year-to-year variability, ± 1 standard deviation for the mean data for the available years is indicated in Fig. 7, although larger deviations in the ship measurements were not shown due significantly to relatively sparse sampling. In the Northern Hemisphere, the annual mean in the upper troposphere is about 0.6–0.8 ppm lower than that in the lower troposphere observed by NOAA/CMDL. A gradual CO_2 decrease with increasing altitude in the Northern Hemisphere is clearly seen around 20°N in comparison to NOAA/CMDL data from Cape Kumukahi (sea level) and Mauna Loa (3.4 km) at Hawaii and our

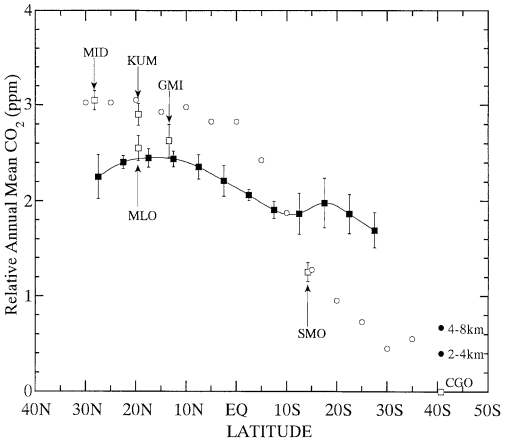

Fig. 7. Average vertical difference of annual mean CO_2 over the Pacific during 1994–1997 in comparison with that in the upper troposphere at 8–13 km from this aircraft observation (closed squares), and middle and lower tropospheres below 8 km observed from the cruise ships between Los Angeles and New Zealand (open circles) and ground-based stations (open squares) by NOAA/CMDL, and aircraft measurements over Australia by CSIRO (closed circles). MID (Sand Island, Midway), KUM (Cape Kumukahi, Hawaii), MLO (Mauna Loa, Hawaii), GMI (Guam, Marianas Islands), SMO (American Samoa), and CGO (Cape Grim, Tasmania) are the observational site codes of NOAA/CMDL. The error bar represents ± 1 standard deviation. Values are represented as a deviation from the CGO.

measurements (8–13 km). In contrast, relatively higher values in the Southern Hemisphere were found in the upper troposphere rather than the lower troposphere. The difference in the CO_2 level between the upper and lower troposphere was about 1 ppm south of 15°S. This negative gradient was also observed in the southern mid-latitudes around 40°S over Australia (Pak, 2000), as shown in Fig. 7. The hemispheric difference in the CO_2 gradient with altitude was consistent with the previous results of vertical profiles from several aircraft observations (Pearman and Beardsmore, 1984; Nakazawa et al., 1991; Matsueda and Inoue, 1996; Pak et al., 1996). In particular, the negative vertical gradient in the Southern Hemisphere could be explained mainly by the southward transport of the northern hemispheric air through the upper troposphere that is primarily driven by the convective processes in the tropical regions (Nakazawa et al., 1991; Matsueda et al., 1993).

This upper tropospheric transport process has also been demonstrated by several 3-D transport model studies (e.g., Taguchi, 1996).

In our comparisons in Fig. 7, the vertical gradient with altitudes was reversed around 10°S as compared with the ship measurements between Los Angeles and New Zealand by NOAA/CMDL. On the other hand, it has been reported that a different latitude around 10°N with an opposite vertical profile was observed when comparing aircraft and ship data over the same area of the western Pacific (Nakazawa et al., 1991). This difference between two cases suggests to be due to different longitudes of the sampling area for the ship measurements, because the both aircraft measurements were made on the similar flight route. It is consistent with our comparison in Fig. 7 because only a small vertical gradient of about 0.1 ppm around 10°N was observed when we compared data from Guam (13°26′N, 144°47′E) and our data collected over the same region of the western Pacific. These results imply that a longitudinal difference in the CO_2 level should be carefully considered when comparisons are made between the upper and lower troposphere over the Pacific. The CO_2 mixing ratios in the lower troposphere have been reported to differ in the western and eastern Pacific regions (Tans et al., 1989; Nakazawa et al., 1992). There are no systematic data for the longitudinal differences in upper tropospheric CO_2 over the Pacific, but a slight difference in upper tropospheric methane has been reported between the western and central Pacific regions (Matsueda et al., 1993). More observational data are needed to clarify the CO_2 distributions with longitude in the upper troposphere.

4.3. *Seasonal cycle*

To extract the seasonal cycle for each latitudinal band, the long-term trend was subtracted from the final fitting curve. Figure 8 shows detrended seasonal cycles for 12 latitudinal bands from 30°N to 30°S averaged from 1994–1998. In the Northern Hemisphere, the average seasonal cycle was the largest at 30°N–25°N with a maximum in early May and a minimum in late September. The cycle rapidly decayed toward the equator with a delay of phase. On the other hand, the seasonal cycle was largely reduced for CO_2 in the Southern Hemisphere, and the pattern differed from the one

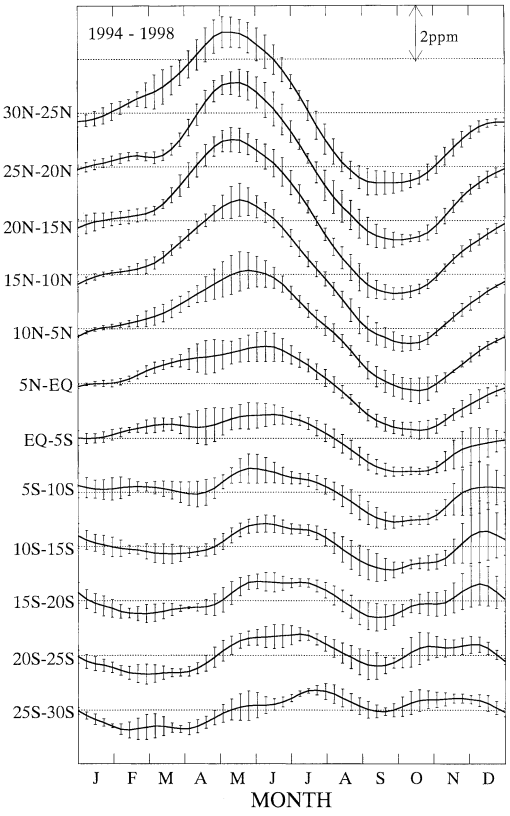

Fig. 8. The mean seasonal cycles for 12 latitudinal bands between 30°N and 30°S at 8–13 km over the Pacific during 1994–1998. The solid line represents the mean seasonality for 5 yr, while the error bars represent a range of ±1 standard deviation.

in the Northern Hemisphere. The seasonality in the Southern Hemisphere showed a relatively complicated variation with double increased peaks around June–July and November–December. No significant change in the seasonal cycle pattern with latitudes was observed in the Southern Hemisphere. These characteristics of averaged CO_2 seasonality in the upper troposphere are quite similar to those found in the previous observations over the same area of the western Pacific (Nakazawa et al., 1991).

Figure 8 also shows ±1 standard deviation for the averaged seasonal cycle for the four or five years during which it was available from 1994 and 1998 in order to show the year-to-year variability in the patterns of the seasonal cycle. Relatively larger deviations in the Northern Hemisphere

appeared during the maximum season for CO_2 around May rather than during the minimum season around September. The larger variability was found to be due to a slightly enhanced CO_2 maximum in 1998. In the Southern Hemisphere, the largest standard deviations of about 1 ppm were found in the latitudes between 5°S and 20°S from November through December. These large deviations in the southern spring season were caused by a significant enhancement of the CO_2 level during the El Niño years of 1997 and 1994. In particular, the southern spring peak in 1997 surpassed the other peak in the southern winter season from around June through July, while the remaining data during the non-El Niño years in 1995 and 1996 showed a different pattern with a larger peak during the southern winter season. The fact that the increased peak in the southern winter season was larger than that in the southern spring season is consistent with previous results in the non-El Niño years in 1984 and 1985 (Nakazawa et al., 1991). These results suggest that a yearly change in the pattern of the seasonal cycle is associated with the ENSO events.

The peak-to-peak amplitude of the seasonal cycle for each latitudinal band was calculated for each year by taking the sum of the maximum and minimum difference in the detrended seasonal cycle (Fig. 9). The amplitude in the Northern Hemisphere showed a rapid decrease from about 6 ppm around 30°N to about 3 ppm at the equator. In the Southern Hemisphere, a relatively lower amplitude of about 2 ppm was observed with a few exceptions in 1997 and 1998. Although a similar decrease of the amplitudes from the Northern to Southern Hemispheres was observed in the previous data for two years over the same area of the western Pacific (Nakazawa et al., 1991), our data for 6 yr represent a year-to-year variability of the amplitude in the upper troposphere. In particular, the amplitude in 1997 showed a large increase in the southern subtropical regions. This increase in 1997 was accompanied by a change in the pattern of the seasonal cycle that showed significant growth in the southern spring peak, as described above. Relatively larger spring peak rather than winter one was found in three latitudinal bands between 5°S and 20°S in 1997. The amplitudes in these subtropical regions showed a large increase to more than 3 ppm, that was calculated from the spring maximum to minimum. On the other hand, amplitudes from the winter maximum to minimum between 5°S and 20°S in 1997 showed relatively lower values around 2 ppm, which was similar to those in other years (Fig. 9). It is suggested that the enhancement of the southern spring peak is responsible for the increased amplitude in the southern subtropics in 1997. In the Northern Hemisphere, a slight increase in the amplitude in 1998 was found in the northern subtropics around 20°N. These results suggest that the increase in amplitude is linked with the change in the pattern of the seasonal cycle during the largest 1997/98 ENSO event. The large deviations in values for 1994 were attributed to a larger error in estimating the CO_2 seasonal peak that occurred as a result of infrequent sampling before June 1994.

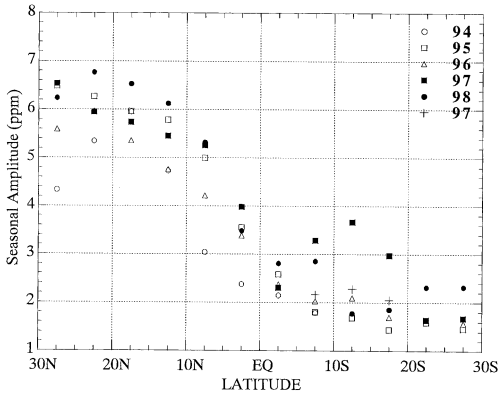

Fig. 9. The peak-to-peak amplitudes of the seasonal cycles for 12 latitudinal bands between 30°N and 30°S during 1994–1998. The crosses represent the amplitudes in 1997 calculated from the southern winter maximum to minimum. The procedure for data analysis is described in detail in the text.

It has been reported that several longer CO_2 records in the surface background air have shown an increase of seasonal amplitude in the Northern Hemisphere at a rate of 0.7–1.3%/yr, which was attributed to possible CO_2 fertilization of the terrestrial biosphere (e.g., Cleveland et al., 1983; Bacastow et al., 1985; Keeling et al., 1985; Keeling et al., 1996b; Myneni et al., 1997). However, no clear trend was found in the upper tropospheric CO_2 data from the western Pacific over a 10-yr period when it was compared to previous measurements for 1984–1985 (Nakazawa et al., 1991) and our own from 1993–1998. It is obvious from the

results in Fig. 9 that the year-to-year variability of the amplitudes is too large for determining a trend as small as the increase in the amplitude in the upper tropospheric record. This is due to relatively sparse sampling and large natural variability.

CO_2 seasonal amplitude in the surface background air showed a north-to-south decrease from about 8–9 ppm around 30°N to about 3 ppm around the equator and a constant value of about 1 ppm in the Southern Hemisphere (Tanaka et al., 1987b; Conway et al., 1988, 1994). These results indicate that the seasonal amplitude around 30°N in the upper troposphere is about 2–3 ppm lower than that of the lower troposphere, but the amplitudes throughout the Southern Hemisphere were about 1 ppm larger in the upper troposphere. This hemispheric difference was consistent with a vertical decrease in the amplitude over Japan in the Northern Hemisphere (Tanaka et al., 1987a; Nakazawa et al., 1993) and a vertical increase over Australia in the Southern Hemisphere (Pearman and Beardsmore, 1984; Pak et al., 1996). It has been suggested that the larger seasonal amplitude in the upper troposphere of the Southern Hemisphere is largely influenced by a rapid transport of northern hemispheric air through the upper layer.

The phase delay of the seasonal cycle was found in the maximum and minimum peaks from 30°N to the equator in the Northern Hemisphere (Fig. 8). To calculate the phase difference with latitudes, the days of downward-zero (DZ) and upward-zero (UZ) crossing of the long-term trend curve were calculated for 12 latitudinal bands, and their means were plotted in Fig. 10. Although there were two DZ and UZ due to double peaks south of 5°S in the Southern Hemisphere, only one DZ and UZ values are shown in Fig. 10. The crossing dates were used because they vary less than the minimum and maximum dates when used as indicators for the phase shift of CO_2 seasonality in the surface background air (e.g., Komhyr et al., 1985; Keeling et al., 1996b). In the Northern Hemisphere, the deviation of the DZ dates was small, within ± 1 week, while the UZ had a somewhat larger deviation. These results suggest that the DZ is useful for accurately determining the mean phase shift in the upper troposphere, although the UZ that appears around January was not well determined due to the flatness of the

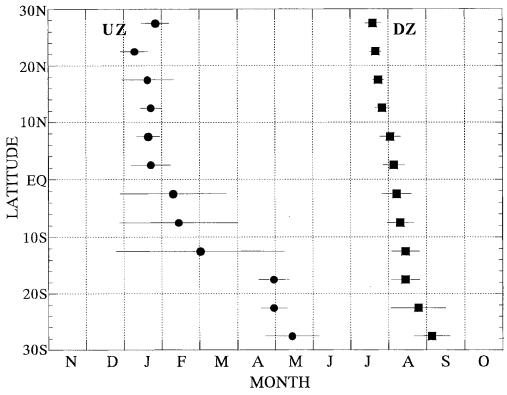

Fig. 10. The latitude dependence of the mean phase of the CO_2 seasonal cycle for 1994–1998. The solid squares and circles represent the mean date of downward-zero (DZ) and upward-zero (UZ) crossing of the long-term trend curve, respectively. The error bar represents ± 1 standard deviation of the mean.

CO_2 buildup in the Northern Hemisphere. The phase difference of the DZ between 30°N and the equator was estimated to be about one month, which is similar to previous observations over the same area of the North Pacific (Nakazawa et al., 1991). The DZ at 20°N was calculated to appear on 23 July in the upper troposphere. Compared with the DZ in Hawaii on a similar latitude, it was reported to be vertically delayed from 11 July at Cape Kumukahi in the lower troposphere to 20 July at Mauna Loa (3.4 km altitude) in the middle troposphere (Conway et al., 1988). These differences indicate that the DZ date was gradually delayed from the lower to the upper troposphere. Such phase delay with an increase in altitude in the Northern Hemisphere was clearly observed in the vertical decay of the seasonal cycle over Japan (Nakazawa et al., 1993). These results suggest that the phase delay with altitudes and latitudes is caused mainly by the propagation of a strong CO_2 seasonal cycle in the surface air in the mid and high latitudes due to photosynthesis and soil respiration.

The DZ in the Southern Hemisphere was delayed toward 30°S, although the deviation was relatively large compared with that in the Northern Hemisphere. This was caused by the yearly change in the pattern of the seasonal cycle during the strong ENSO event, as stated above. The DZ across the equator showed no

significant gap from the Northern to Southern Hemispheres. This result suggested that the CO_2 seasonal signal in the Northern Hemisphere was propagated into the Southern Hemisphere due to a rapid upward air motion combined with a horizontal transport through the upper troposphere. In contrast, it has been reported that the seasonality in the lower troposphere of the Southern Hemisphere was 6 months out of phase with that of the Northern Hemisphere (Tanaka et al., 1987b; Conway et al., 1988). This difference implied that the interhemispheric propagation of the CO_2 seasonal signal across the Intertropical Convergence Zone was faster through the upper troposphere than through the lower troposphere. More detailed interpretation for the propagation process of the CO_2 seasonality over the western Pacific was reported by Nakazawa et al. (1991).

4.4. *Influence of biomass burning*

Biomass burning in the tropics is an important source of atmospheric CO_2 and other trace gases (e.g., Crutzen and Andreae, 1990). The impact of the emissions from biomass burning on the variation of atmospheric CO_2 was examined with three-dimensional models (Iacobellis et al., 1994; Wittenberg et al., 1998); however, the influence of biomass burning on the interannual variability in the upper troposphere was not clarified in detail. From our airliner observations, the long-term records of CO measurements were identified as useful indicators for measuring the annual change that occurs as a result of direct injection of biomass-burning products in the upper troposphere (Matsueda et al., 1998, 1999). Thus, we used the CO data to evaluate the influence of biomass burning on CO_2 variability, according to a procedure that is described in the following section.

First, the overall average of CO from 1993 through 1999 was calculated and subtracted from the observed CO data. The positive CO data from this subtraction are plotted in Fig. 11a to show the excess CO in the Northern (30°N–0°) and Southern (30°S–0°) Hemispheres, while the negative CO data are plotted as zero because they are not needed in the following calculation. The excess CO in the Southern Hemisphere clearly represented a seasonal increase around October of every year and an interannual variation with a large enhancement up to 120 ppb in 1997. Since CO

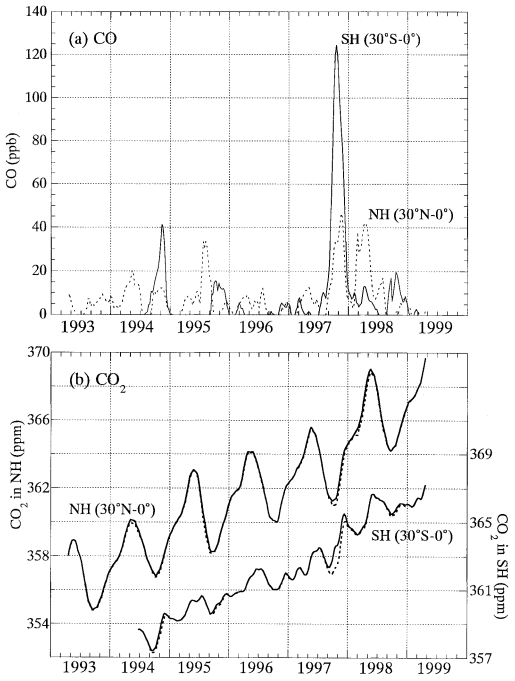

Fig. 11. (a) The time variation of excess CO in the Northern (dashed line) and Southern (solid line) tropics calculated from the observed CO at 8–13 km over the western Pacific during 1993–1999. The excess CO data were defined as the data above the overall average during this observational period of time. (b) The difference of CO_2 time variations between the observation (solid line) and calculated data without biomass-burning CO_2 (dashed line) in the Northern and Southern tropics. The biomass-burning CO_2 was estimated on the basis of the excess CO in (a). The detailed procedure for the data analysis is described in the text.

from biomass burning is emitted largely during the tropical dry season from August to November (Andreae, 1993), the increase of the excess CO in the Southern Hemisphere can be mostly attributed to tropical biomass burning. On the other hand, the excess data of the Northern Hemisphere showed an increase in CO due to biomass burning around October, although an excess amount of CO also appeared in the remaining seasons. This result suggests that the source of the excess CO in the Northern Hemisphere may include not only biomass burning but also some fossil-fuel burning. However, the excess CO due probably to fossil-fuel burning was less than 20 ppb, which suggests that it had an insignificant effect on the estimation

of the influence of biomass-burning CO_2. One exceptional increase to about 40 ppb from February through May of 1998 was noted and attributed to biomass burning that was probably due to prolonged peat land fires in Kalimantan, Indonesia. Second, the excess CO that was considered to be the result of biomass burning was converted into a corresponding increase in CO_2 on the basis of an emission ratio of 10 for CO_2 to CO in tropical biomass burnings (Crutzen and Andreae, 1990). This calculation for the conversion to biomass-burning CO_2 included several uncertainties such as a wide range in the emission ratios and a change in the CO_2/CO ratio during transport due mainly to the oxidation loss of CO. Finally, the CO_2 converted from the excess CO was subtracted from the observed data to obtain CO_2 data that were separate from the influence of biomass burning (Fig. 11b). A difference between the observed CO_2 and the calculated data without biomass burning showed a year-to-year change because biomass-burning emissions were strongly related to the ENSO events (Matsueda et al., 1999). The most significant impact on the CO_2 time variation was found during the strong El Niño event in 1997/98 due to largely enhanced injections of biomass burning into the upper troposphere.

The calculated data were further analyzed without including the CO_2 from the biomass burning in order to examine the influence of biomass burning on the growth rate and annual mean value. Figure 12a compares the CO_2 growth rates showing the observed and calculated data without the influence of biomass burning. The growth rate maximum in the calculated data appeared in early 1998, and its phase was delayed for 2–3 months, as compared with an earlier peak around late 1997 in the observed data. This is similar to the appearance of the growth rate peak observed around early 1998 in the surface air at the JMA monitoring stations in the western North Pacific (Watanabe et al., 2000). These results suggested that the direct injection of CO_2 from biomass burning led to an earlier increase in the growth rate in the upper troposphere rather than in the lower troposphere. No significant difference in the growth rate maximum around 1997/98 was found between the calculated and observed CO_2 data. Figure 12b shows the latitudinal distribution of the annual mean CO_2 compared between the

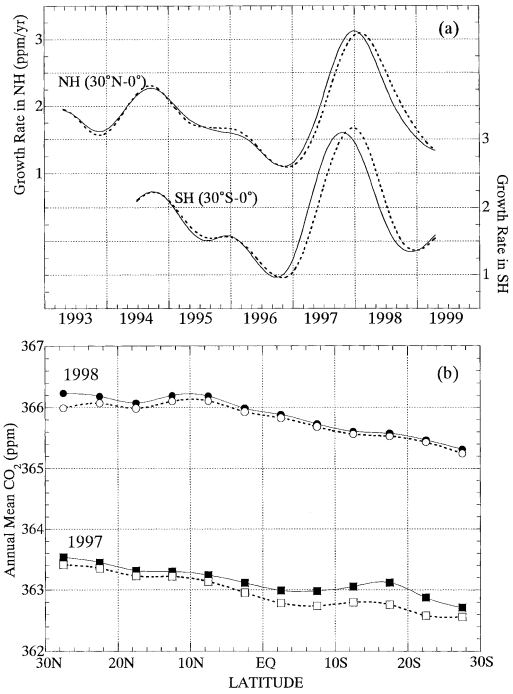

Fig. 12. (a) The difference of CO_2 growth rates between the observed data (solid line) and the calculated data without biomass-burning CO_2 (dashed line) in the Northern and Southern tropics. (b) The difference of latitudinal distribution of annual mean CO_2 between the observed data (solid line) and the calculated data without biomass-burning CO_2 (dashed line).

observed and calculated data in 1997 and 1998. A more significant difference in the latitudinal distribution was found in 1997 than in 1998. The CO_2 increase due to the influence of biomass burning in 1997 was estimated to be about 0.3–0.4 ppm in the Southern Hemisphere and about 0.1 ppm in the Northern Hemisphere. These increases contributed to a change in the distribution of CO_2 with a relatively flat north-to-south gradient in the observed data in 1997. In addition, we found that the seasonal cycle pattern in 1997 was also changed. A largely enhanced spring maximum in 1997 was observed in the Southern Hemisphere as stated above, but the spring and winter maxima in the calculated data were almost the same. These results from the present analysis suggest that the direct input of the biomass burning during the 1997/1998 ENSO event affects the temporal and spatial variations of CO_2 in the upper troposphere.

Although several uncertainties still remain in our estimation, more significant influences were expected because indirect CO_2 production by oxidation of CO and other trace gases emitted from biomass burnings was not considered in the present study. It will be necessary to evaluate quantitatively the effect of biomass burning in more depth by use of a chemical transport model.

5. Conclusions

We observed CO_2 mixing ratios at 8–13 km over the western Pacific to clarify the long-term trend, annual mean, and seasonal cycle from 1993 to 1999. The CO_2 time variations averaged for 6 yr were quite similar to those from previous observations for 1984 and 1985 over the same part of the western Pacific, as reported by Nakazawa et al. (1991). These upper tropospheric data were compared with the surface air data to clarify vertical differences in CO_2 time variations between the upper and lower troposphere. Since the upper tropospheric data will be useful for validating the CO_2 transport model, all of the measurements in the present study will be submitted to the World Data Center for Greenhouse Gases of the World Meteorological Organization (WMO/WDCGG)
(http://gaw.kishou.go.jp/wdcgg.html).

The 6-yr record also showed several characteristics of CO_2 interannual variability in the upper troposphere. The most significant year-to-year change was found in an anomalous increase in the CO_2 growth rate during 1997/98 that was associated with the strong El Niño event. In this ENSO event, changes in latitudinal distribution of the annual mean and seasonal cycle were found when the data were compared to data of non-El Niño years. Such interannual variability suggests a yearly change of CO_2 fluxes from the land biosphere and the ocean as well as the modulation of CO_2 transport from the surface to the upper troposphere. Another possible cause discussed here was the burning of biomass in the tropics, which was largely enhanced during the 1997/98 ENSO events (Matsueda et al., 1999). More observational data for a longer period of time linked with a quantitative evaluation using three-dimensional models will be necessary for a better understanding of CO_2 interannual variability in the upper troposphere.

6. Acknowledgments

We thank the many crew members and ground operation staff of Japan Airlines for their kind cooperation in obtaining the air samples. We are also grateful to Akira Kudo for his technical support with the air sampling system and to Kayoko Nakai for her assistance with the trace gas measurements. We are thankful to two anonymous reviewers for many valuable comments on this manuscript. The JAL Foundation supported the aircraft observation program financially.

REFERENCES

Anderson, B. E., Collins, J. E., Sachse, G. W., Whiting, G. W., Blake, D. R. and Rowland, F. S. 1993. AASE-II observations of trace carbon species distributions in the mid to upper troposphere. *Geophys. Res. Lett.* **20**, 2539–2542.

Anderson, B. E., Gregory, G. L., Collins Jr., J. E., Sachse, G. W., Conway, T. J. and Whiting, G. P. 1996. Airborne observations of spatial and temporal variability of tropospheric carbon dioxide. *J. Geophys. Res.* **101**, 1985–1997.

Andreae, M. O. 1993. Global distribution of fires seen from space (abstract). *Eos Trans. AGU* **74**, 129–135.

Bacastow, R. B. 1976. Modulation of atmospheric carbon dioxide by the Southern Oscillation. *Nature* **261**, 116–118.

Bacastow, R. B., Adams, J. A., Keeling, C. D., Moss, D. J. and Whorf, T. P. 1980. Atmospheric carbon dioxide, the Southern Oscillation, and the weak 1975 El Niño. *Science* **210**, 66–68.

Bacastow, R. B., Keeling, C. D. and Whorf, T. P. 1985. Seasonal amplitude increase in atmospheric CO_2 concentration at Mauna Loa, Hawaii, 1959–1982. *J. Geophys. Res.* **90**, 10,529–10,540.

Battle, M., Bender, M. L., Tans, P. P., White, J. W. C., Ellis, J. T., Conway, T. and Francey, R. J. 2000. Global carbon sinks and their variability inferred from atmospheric O_2 and $\delta^{13}C$. *Science* **287**, 2467–2470.

Bell, G. D., Halpert, M. S., Ropelewski, C. F., Kousky, V. E., Douglas, A. V., Schnell, R. C. and Gelman, M. E. 1999. Climate assessment for 1998. *Bull. Am. Meteorol. Soc.* **80**, S1–S48.

Bischof, W. 1962. Variations in concentration of carbon dioxide in the free troposphere. *Tellus* **14**, 87–90.

Bischof, W. 1971. Carbon dioxide in the upper troposphere and lower stratosphere. II. *Tellus* **23**, 558–561.

Bischof, W., Borchers, R., Fabian, P. and Krüger, B. C. 1985. Increased concentration and vertical distribution of carbon dioxide in the stratosphere. *Nature* **316**, 708–710.

Boering, K. A., Wofsy, S. C., Daube, B. C., Schneider, H. R., Loewenstein, M., Podolske, J. R. and Conway, T. J. 1996. Stratospheric mean ages and transport rates from observations of carbon dioxide and nitrous oxide. *Science* **274**, 1340–1343.

Bolin, B. and Bischof, W. 1970. Variations of the carbon dioxide content of the atmosphere in the northern hemisphere. *Tellus* **22**, 431–442.

Bousquet, P., Peylin, P., Ciais, P., Le Quéré, C., Friedlingstein, P. and Tans, P. P. 2000. Regional changes in carbon dioxide fluxes of land and oceans since 1980. *Science* **290**, 1342–1346.

Brenninkmeijer, C. A. M., Crutzen, P. J., Fischer, H., Güsten, H., Hans, H., Heinrich, G., Heintzenberg, J., Hermann, M., Immelmann, T., Kersting, D., Maiss, M., Nolle, M., Pitscheider, A., Pohlkamp, H., Scharffe, D., Specht, K. and Wiedensohler, A. 1999. CARIBIC — Civil aircraft for global measurement of trace gases and aerosols in the tropopause region. *J. Atmos. Oceanic Technol.* **16**, 1373–1383.

Cleveland, W. S., Freeny, A. E. and Graedel, T. E. 1983. The seasonal component of atmospheric CO_2: information from new approaches to the decomposition of seasonal time series. *J. Geophys. Res.* **88**, 10,934–10,946.

Conway, T. J. and Steele, L. P. 1989. Carbon dioxide and methane in the Arctic atmosphere. *J. Atmos. Chem.* **9**, 81–99.

Conway, T. J., Raatz, W. E. and Gammon, R. H. 1985. Airborne CO_2 measurements in the Arctic during spring 1983. *Atmos. Environ.* **19**, 2195–2201.

Conway, T. J., Tans, P., Waterman, L. S., Thoning, K. W., Masarie, K. A. and Gammon, R. H. 1988. Atmospheric carbon dioxide measurements in the remote global troposphere, 1981–1984. *Tellus* **40B**, 81–115.

Conway, T. J., Tans., P. P., Waterman, L. S., Thoning, K. W., Kitzis, D. R., Masarie, K. A. and Zhang, N. 1994. Evidence for interannual variability of the carbon cycle from the National Oceanic and Atmospheric Administration/Climate Monitoring and Diagnostics Laboratory global air sampling network. *J. Geophys. Res.* **99**, 22,831–22,855.

Craig, S. G., Holmén, K. J., Bonan, G. B. and Rasch, P. J. 1998. Atmospheric CO_2 simulated by the National Center for Atmospheric Research Community Climate Model 1. Mean fields and seasonal cycles. *J. Geophys. Res.* **103**, 13,213–13,235.

Crutzen, P. J. and Andreae, M. O. 1990. Biomass burning in the tropics: impact on atmospheric chemistry and biogeochemical cycles. *Science* **250**, 1669–1678.

Elliott, W. P., Angell, J. K. and Thoning, K. W. 1991. Relation of atmospheric CO_2 to tropical sea and air temperatures and precipitation. *Tellus* **43B**, 144–155.

Fan, S., Gloor, M., Mahlman, J., Pacala, S., Sarmiento, J., Takahashi, T. and Tans, P. 1998. A large terrestrial carbon sink in North America implied by atmospheric and oceanic carbon dioxide data and models. *Science* **282**, 442–446.

Feely, R. A., Wanninkhof, R., Takahashi, T. and Tans, P. 1999. Influence of El Niño on the equatorial Pacific contribution to atmospheric CO_2 accumulation. *Nature* **398**, 597–601.

Francey, R. J., Tans, P. P., Allison, C. E., Enting, I. G., White, J. W. C. and Trolier, M. 1995. Changes in oceanic and terrestrial carbon uptake since 1982. *Nature* **373**, 326–330.

Harnisch, J., Bischof, W., Borchers, R., Fabian, P. and Maiss, M. 1998. A stratospheric excess of CO_2 — due to tropical deep convection? *Geophys. Res. Lett.* **25**, 63–66.

Hintsa, E. J., Boering, K. A., Weinstock, E. M., Anderson, J. G., Gary, B. L., Pfister, L., Daube, B. C., Wofsy, S. C., Loewenstein, M., Podolske, J. R., Margitan, J. J. and Bui, T. P. 1998. Troposphere-to-stratosphere transport in the lowermost stratosphere from measurements of H_2O, CO_2, N_2O and O_3. *Geophys. Res. Lett.* **25**, 2655–2658.

Iacobellis, S. F., Frouin, R., Razafimpanilo, H., Somerville, R. C. J. and Piper S. C. 1994. North Africa savanna fires and atmospheric carbon dioxide. *J. Geophys. Res.* **99**, 8321–8334.

Inoue, H. Y., Ishii, M., Matsueda, H. and Ahoyama, M. 1996. Changes in longitudinal distribution of the partial pressure of CO_2 (pCO_2) in the central and western equatorial Pacific, west of 160°W. *Geophys. Res. Lett.* **23**, 1781–1784.

Japan Meteorological Agency (JMA) 1999. Monthly Report on *Climate System No. 99-11* (ed. JMA). JMA, Tokyo.

Keeling, C. D., Harris, T. B. and Wilkins, E. M. 1968. Concentration of atmospheric carbon dioxide at 500 and 700 millibars. *J. Geophys. Res.* **73**, 4511–4528.

Keeling, C. D., Whorf, T. P., Wong, C. S. and Bellagay, R. D. 1985. The concentration of atmospheric carbon dioxide at Ocean Weather Station P from 1969 to 1981. *J. Geophys. Res.* **90**, 10,511–10,528.

Keeling, C. D., Bacastow, R. B., Carter, A. F., Piper, S. C. Whorf, T. P., Heimann, M., Mook, W. G. and Roeloffzen, H. 1989. A three-dimensional model of atmospheric CO_2 transport based on observed winds. (1) Analysis of observational data. In: *AGU Monograph* **55**. American Geophysical Union, Washington, USA, 165–362.

Keeling, C. D., Whorf, T. P., Wahlen, M. and van der Plicht, J. 1995. Interannual extremes in the rate of rise of atmospheric carbon dioxide since 1980. *Nature* **375**, 666–670.

Keeling, C. D., Chin, J. F. S. and Whorf, T. P. 1996. Increased activity of northern vegetation inferred from atmospheric CO_2 measurements. *Nature* **382**, 146–149.

Komhyr, W. D., Gammon, R. H., Harris, T. B., Waterman, L. S., Conway, T. J., Taylor, W. R. and Thoning,

K. W. 1985. Global atmospheric CO_2 distribution and variations from 1968–1982 NOAA/GMCC CO_2 flask sampling data. *J. Geophys. Res.* **90**, 5567–5596.

Law, R. and Simmonds, I. 1996. The sensitivity of deduced CO_2 sources and sinks to variations in transport and imposed surface concentrations. *Tellus* **48B**, 613–625.

Lee, K., Wanninkhof, R., Takahashi, T., Doney, S. C. and Feely, R. A. 1998. Low interannual variability in recent oceanic uptake of atmospheric carbon dioxide. *Nature* **396**, 155–159.

Matsueda, H., Inoue, H. Y. and Ishii, M. 1993. Latitudinal distributions of methane in the upper troposphere and marine boundary air over the Pacific in 1990. *Geophys. Res. Lett.* **20**, 695–698.

Matsueda, H. and Inoue, H. Y. 1996. Measurements of atmospheric CO_2 and CH_4 using a commercial airliner from 1993 to 1994. *Atmos. Environ.* **30**, 1647–1655.

Matsueda, H., Inoue, H. Y., Sawa, Y., Tsutsumi, Y. and Ishii, M. 1998. Carbon monoxide in the upper troposphere over the western Pacific between 1993 and 1996. *J. Geophys. Res.* **103**, 19,093–19,110.

Matsueda, H., Inoue, H. Y., Ishii, M. and Tsutsumi, Y. 1999. Large injection of carbon monoxide into the upper troposphere due to intense biomass burning in 1997. *J. Geophys. Res.* **104**, 26,867–26,879.

Murayama, S., Nakazawa, T., Yamazaki, K., Aoki, S., Makino, Y., Shiobara, M., Fukabori, M., Yamanouchi, T., Shimizu, A., Hayashi, M., Kawaguchi, S. and Tanaka, M. 1995. Concentration variations of atmospheric CO_2 over Syowa Station, Antarctica and their interpretation. *Tellus* **47B**, 375–390.

Myneni, R. B., Keeling, C. D., Tucker, C. J., Asrar, G. and Nemani, R. R. 1997. Increased plant growth in the northern high latitudes from 1981 to 1991. *Nature* **386**, 698–702.

Nakazawa, T., Miyashita, K., Aoki, S. and Tanaka, M. 1991. Temporal and spatial variations of upper tropospheric and lower stratospheric carbon dioxide. *Tellus* **43B**, 106–117.

Nakazawa, T., Murayama, S., Miyashita, K., Aoki, S. and Tanaka, M. 1992. Longitudinally different variations of lower tropospheric carbon dioxide concentrations over the North Pacific Ocean. *Tellus* **44B**, 161–172.

Nakazawa, T., Morimoto, S., Aoki, S. and Tanaka, M. 1993. Time and space variations of the carbon isotopic ratio of tropospheric carbon dioxide over Japan. *Tellus* **45B**, 258–274.

Nakazawa, T., Machida, T., Sugawara, S., Murayama, S., Morimoto, S., Hashida, G., Honda, H. and Itoh, T. 1995. Measurements of the stratospheric carbon dioxide concentration over Japan using a balloon-borne cryogenic sampler. *Geophys. Res. Lett.* **22**, 1229–1232.

Nakazawa, T., Sugawara, S., Inoue, G., Machida, T., Makshyutov, S. and Mukai, H. 1997a. Aircraft measurements of the concentrations of CO_2, CH_4, N_2O and CO and the carbon and oxygen isotopic ratios of CO_2 in the troposphere over Russia. *J. Geophys. Res.* **102**, 3843–3859.

Nakazawa, T., Morimoto, S., Aoki, S. and Tanaka, M. 1997b. Temporal and spatial variations of the carbon isotopic ratio of atmospheric carbon dioxide in the western Pacific region. *J. Geophys. Res.* **102**, 1271–1285.

Pak, B. C., Langenfelds, R. L., Francey, R. J., Steele, L. P. and Simmonds, I. 1996. A climatology of trace gases from the Cape Grim over-flights, 1992–1995. In: *Baseline Atmospheric Program Australia 1994–95* (eds. R. J. Francey, A. L. Dick and N. Derek). Bureau of Meteorology and CSIRO Devision of Atmospheric Research, Australia, 41–52.

Pak, B. C. 2000. Vertical structure of atmospheric trace gases over southeast Australia. PhD Thesis, University of Melbourne, 59–72.

Pearman, G. I. and Garratt, J. R. 1973. Space and time variations of tropospheric carbon dioxide in the southern hemisphere. *Tellus* **25**, 309–311.

Pearman, G. I. and Beardsmore D. J. 1984. Atmospheric carbon dioxide measurements in the Australian region: Ten years of aircraft data. *Tellus* **36B**, 1–24.

Ray, E. A., Moore, F. L., Elkins, J. W., Dutton, G. S., Fahey, D. W., Vömel, H., Oltmans, S. J. and Rosenlof, K. H. 1999. Transport into the Northern Hemisphere lowermost stratosphere revealed by in situ tracer measurements. *J. Geophys. Res.* **104**, 26,565–26,580.

Rayner, P. J., Enting, I. G., Francey, R. J. and Langenfelds, R. 1999a. Reconstructing the recent carbon cycle from atmospheric CO_2, $\delta^{13}C$ and O_2/N_2 observations. *Tellus* **51B**, 213–232.

Rayner, P. J., Law, R. M. and Dargaville, R. 1999b. The relationship between tropical CO_2 fluxes and the El Niño–Southern Oscillation. *Geophys. Res. Lett.* **26**, 493–496.

Schmidt, U. and Khedim, A. 1991. In situ measurements of carbon dioxide in the winter Arctic vortex and at midlatitudes: an indicator of the 'age' of stratospheric air. *Geophys. Res. Lett.* **18**, 763–766.

Strahan, S. E., Douglass, A. R., Nielsen, J. E. and Boering, K. A. 1998. The CO_2 seasonal cycle as a tracer of transport. *J. Geophys. Res.* **103**, 13,729–13,741.

Strunk, M., Engel, A., Schmidt, U., Volk, C. M., Wetter, T., Levine, I. and Glatzel-Mattheier, H. 2000. CO_2 and SF_6 as stratospheric age tracers: consistency and the effect of mesospheric SF_6-loss. *Geophys. Res. Lett.* **27**, 341–344.

Taguchi, S. 1996. A three-dimensional model of atmospheric CO_2 transport based on analyzed winds: model description and simulation results for TRANSCOM. *J. Geophys. Res.* **101**, 15,099–15,109.

Tanaka, M., Nakazawa, T. and Aoki, S. 1987a. Time and space variations of tropospheric carbon dioxide over Japan. *Tellus* **39B**, 3–12.

Tanaka, M., Nakazawa, T. and Aoki, S. 1987b. Seasonal and meridional variations of atmospheric carbon dioxide in the lower troposphere of the northern and southern hemispheres. *Tellus* **39B**, 29–41.

Tans, P. P., Conway, T. J. and Nakazawa, T. 1989. Latitudinal distribution of the sources and sinks of atmospheric carbon dioxide derived from surface observations and an atmospheric transport model. *J. Geophys. Res.* **94**, 5151–5172.

Tans, P. P., Bakwin, P. S., Conway, T. J., Dissly, R. W., Dlugokencky, E. J., Geller, L. S., Guenther, D. W., Hurst, D. F., Kitzis, D. R., Lang, P. M., Masarie, K. A., Miller, J. B., Novelli, P. C., Prostko-Bell, C., Ramonet, M., Thoning, K. W., Trolier, M., Waterman, L. S., Zhang, N. and Zhao, C. 1996. Carbon cycle. In: *Climate monitoring and diagnostics laboratory summary report No. 23*, 1994–95 (eds. D. J. Hofmann, J. T. Peterson and R. M. Rosson). US Department of Commerce, 29–49.

Tans, P. P., Bakwin, P. S., Bruhwiler, L., Conway, T. J., Dlugokencky, E. J., Guenther, D. W., Hurst, D. F., Kitzis, D. R., Lang, P. M., Masarie, K. A., Miller, J. B., Novelli, P. C., Prostko-Bell, C., Thoning, K. W., Vaughn, B. H., White, J. W. C., Yakir, D. and Zhao, C. 1998. Carbon cycle. In: *Climate monitoring and diagnostics laboratory summary report No. 24*, 1996–1997 (eds. D. J. Hofmann, J. T. Peterson and R. M. Rosson). US Department of Commerce, 30–51.

Thompson, M. L., Enting, I. G., Pearman, G. I. and Hyson, P. 1986. Interannual variation of atmospheric CO_2 concentration. *J. Atmos. Chem.* **4**, 125–155.

Waliser, D. E. and Gautier, C. 1993. A satellite-derived climatology of the ITCZ. *J. Climate* **6**, 2162–2174.

Watanabe, F., Uchino, O., Joo, Y., Aono, M., Higashijima, K., Hirano, Y., Tsuboi, K. and Suda, K. 2000. Interannual variation of growth rate of atmospheric carbon dioxide concentration observed at the JMA's three monitoring stations: large increase in concentration of atmospheric carbon dioxide in 1998. *J. Meteor. Soc. Jpn* **78**, 673–682.

Wessel, P. and Smith, W. H. F. 1991. Free software helps map and display data. *EOS Trans. AGU* **72**, 445–446.

Wittenberg, U., Heimann, M., Esser, G., McGuire, A. D. and Sauf, W. 1998. On the influence of biomass burning on the seasonal CO_2 signal as observed at monitoring stations. *Glob. Biogeochem. Cyc.* **12**, 531–544.

Wofsy, S. C., Harriss, R. C. and Kaplan, W. A. 1988. Carbon dioxide in the atmosphere over the Amazon Basin. *J. Geophys. Res.* **93**, 1377–1387.

Zahn, A., Neubert, R., Maiss, M. and Platt, U. 1999. Fate of long-lived trace species near the Northern Hemispheric tropopause: carbon dioxide, methane, ozone, and sulfur hexafluoride *J. Geophys. Res.* **104**, 13,923–13,942.